metals

Article

Machine Learning-Based Multi-Objective Optimization for Enhancing the Performance of Block Support Structures for Electron Beam Additive Manufacturing

Mustafa M. Nasr [1], Wadea Ameen [2,*], Abdulmajeed Dabwan [1] and Abdulrahman Al-Ahmari [3,4]

[1] Industrial Engineering Department, College of Engineering, Taibah University, Medina 41411, Saudi Arabia; mmnasr@taibahu.edu.sa (M.M.N.); adabwan@taibahu.edu.sa (A.D.)
[2] Industrial Engineering Department, College of Engineering, Alyamamah University, Riyadh 11512, Saudi Arabia
[3] Industrial Engineering Department, College of Engineering, King Saud University, Riyadh 11421, Saudi Arabia; alahmari@ksu.edu.sa
[4] Raytheon Chair for Systems Engineering (RCSE Chair), Advanced Manufacturing Institute, King Saud University, Riyadh 11421, Saudi Arabia
* Correspondence: w_qaid@yu.edu.sa

Abstract: Electron beam melting (EBM) technology has gained prominence owing to its ability to enhance production efficiency and meet green manufacturing standards. However, overhang structures are a significant issue for additive manufacturing due to their need for supporting structures during printing. This increases manufacturing time, requiring more material, extra effort, and a more complex engineering procedure. Therefore, this research aims to develop an intelligent optimization method based on AI-ANFIS/Al-ANN and improved NSGA-III, integrating the AM design, 3D printing, and post-processing phases to enhance the performance of block support structures and the quality of the EBM parts produced. To achieve this, statistical analysis was performed to detail the simultaneous influence of block support type, block support structure design, and EBM parameters on fabricating performance, warping deformation, support removal time, and support volume. After that, intelligent models based on ANFIS/ANN and the advanced NSGA-III method were developed for monitoring and optimizing the performance of specified block support structures. The results reveal that the block support type, block support structure design, and EBM parameters simultaneously significantly affect block support structures' performance. This study illustrated that the AI models based on ANFIS might provide more accurate and reliable estimation models for monitoring and predicting support volume, support removal time, and warping deformation, exhibiting reduced errors of 0.992%, 1.2%, 1.28%, and 1.06%, respectively, in comparison to empirical measurements, ANN models, and regression models. Finally, the developed intelligent method obtains the optimal block support type, block support design, and EBM parameters to enhance the quality of produced parts, reduce material wastage, and reduce the post-processing time of fabricated EBM Ti6Al4V. Henceforth, smart systems may be employed to create innovative solutions that integrate the AM design, 3D printing, and post-processing stages. This will allow for the monitoring and improvement of AM process performance, as well as the fulfillment of Industry 4.0 requirements.

Keywords: electron beam additive manufacturing; block support structures' performance; statistical analysis; intelligent system; ANFIS; ANN; NSGA-III method

check for updates

Academic Editor: David Bourell

Received: 23 April 2025
Revised: 3 June 2025
Accepted: 10 June 2025
Published: 17 June 2025

Citation: Nasr, M.M.; Ameen, W.; Dabwan, A.; Al-Ahmari, A. Machine Learning-Based Multi-Objective Optimization for Enhancing the Performance of Block Support Structures for Electron Beam Additive Manufacturing. *Metals* **2025**, *15*, 671. https://doi.org/10.3390/met15060671

Copyright: © 2025 by the authors. Licensee MDPI, Basel, Switzerland. This article is an open access article distributed under the terms and conditions of the Creative Commons Attribution (CC BY) license (https://creativecommons.org/licenses/by/4.0/).

1. Introduction

Additive manufacturing (AM) generally includes a range of technologies that fabricate products layer by layer from a digital three-dimensional model. Additive manufacturing technologies are more efficient for producing complex parts in small quantities where traditional manufacturing techniques would incur significant lead times and material waste. However, a major issue with additive manufacturing (AM) and electron beam melting (EBM) in particular is the building of structures with overhanging parts. That is because overhanging surfaces require supporting structures when the part is built. Support structures are essential for sustaining overhanging elements in nearly all AM methods. Support structures are generated according to the part's specifications during the pre-processing phase. In the post-processing phase, support structures are removed using various processes, including chemical, mechanical, and thermal methods, among others [1,2]. The SG + module in Magics software is utilized for the design and fabrication of support structures. The SG + module provides many forms of support, including points, webs, blocks, and contour, as seen in Figure 1. The block support structure is ideal for large volumetric parts, point support is suitable for small features, web support is used for circular areas, and line support structures are applied in narrow downward-facing locations. The block contour support structure was utilized to improve the stability of object contours during metal sintering [1].

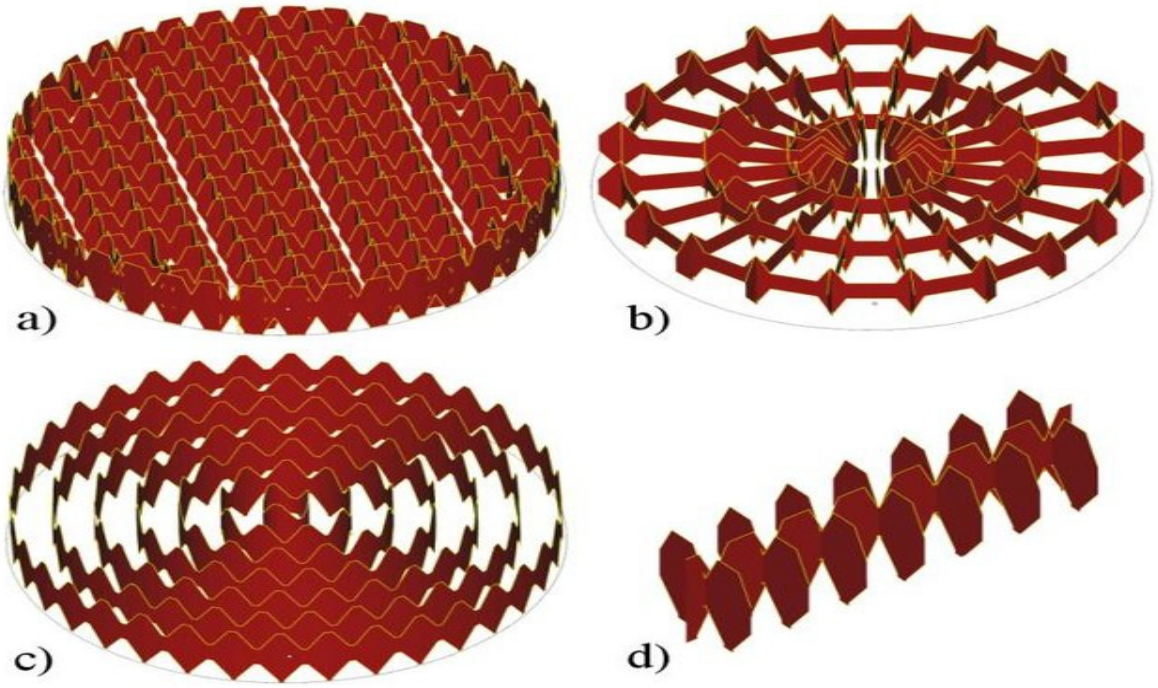


Figure 1. Different support structures: (**a**) block, (**b**) web, (**c**) contour, (**d**) line {shape and size accuracy of 3D-printed AlSi12 parts}.

Automated support generated by software, particularly block support, often fails to accommodate complicated geometries and generally overestimates support thickness. Furthermore, it is inadequate for retrieving the raw loose powder that becomes ensnared in the support structures throughout the construction process [3]. Block support structures possess numerous design parameters that can influence the performance of the final parts. Several researchers have paid attention to the design and optimization of the support structure of metal additive manufacturing, for instance. Jiang et al. [4] developed a support generation technique via print path planning to minimize support material usage in additive manufacturing parts with flat features. In their study, two parts were produced

using the proposed technique, resulting in significantly reduced support material usage compared to conventional line and grid support production methods. The results demonstrate the efficacy of this support generation approach in lowering both support usage and surface degradation, hence rendering additive manufacturing a more environmentally friendly and sustainable production technology. Ameen et al. [5] examined how different process parameters and support design aspects impacted the cost and quality of the support structures used in printing the EBM Ti6Al4V part. The findings indicate that the design and process parameters of the support significantly impact the support volume and accuracy of overhangs. The most significant deformations linked to overhang manufacturing were shown to be warping and side loss deformations. Shen [6] proposed a method for generating bridge support structures that may reduce material usage by around 15.19% and time by 24.41% compared to traditional vertical support structures. Calig-nano [7] studied the manufacturability of overhanging structures using improved support parts for aluminum and titanium alloys. They executed an experimental investigation to determine the optimum self-supporting overhanging structures utilizing the Taguchi L36 design methodology. The findings showed that non-assembly mechanisms with overhang surfaces may be built with optimum support. They also recommended that to achieve the optimal balance between accuracy, cost, and production time, it is important to orient the item appropriately in the SLM machine to build it with minimal support structure.

Support structures are a significant issue in additive manufacturing, increasing production time, material usage, effort, processing time, and post-processing costs. Several research attempts have been made to address these issues. For example, Ameen et al. [8] studied the influence of EBM process parameters (current, scan speed, line offset, and focus offset) on warping deformation. They found that a scan speed of 4530 mm/s, a focus offset of 3 mm, a line offset of 0.3 mm, and a current of 15 mA obtained the lowest deformation at 0.28 mm. Vaidya and Anand [9] utilized Dijkstra's shortest-path method [10] to develop cellular support structures that reduce support volume. They employed a numerical model to demonstrate the capability of the proposed approaches. Their case studies demonstrate a significant reduction in support volume, sintered area, and support contact area as compared to totally solid support, while adequately accounting for support accessibility during post-processing. Järvinen et al. [11] evaluated the usefulness of two support structure designs, namely, web and tube support, for the LAM of stainless steel in two industrial applications: one for dentistry and another for jewelry use. The results show that the removability of the web support type was much superior to that of the tube support type. In addition, it was found that support structures are crucial to the LAM process, significantly influencing both manufacturability and the final quality of the part. Lindecke et al. [12] investigated the tensile strength of the connection between support structures and the SLM TiAl6V4 parts for different support structures. The findings indicate that standard block support structures yield an average actual support strength of around 269 MPa, representing a significant decrease from the solid material's strength of 1286 MPa. Allen and Dutta [13] delineated a method for ascertaining the orientation necessary for fabricating an item with minimum support systems. The algorithm selects the optimal orientation from a collection of potential orientations. For example, if two orientations necessitate support structures with identical contact surface areas, the orientation with the lower center of mass is selected. It is improbable that the two orientations would possess a support structure with similar contact areas. Wei et al. [14] proposed a model decomposition strategy utilizing genetic algorithm optimization for identifying overhang regions and support-related overhang regions to enhance the precision of overhang identification and printing accuracy in fused filament fabrication (FFF). The findings indicated that the

suggested approach for producing support structures might decrease material consumption by 27%.

Many researchers have suggested various designs and optimizations of support structure design. Poyraz et al. [15] examined several support structure designs and applied them to a thin-walled IN625 part fabricated by DMLS. To accurately portray extreme situations, they conducted two tests on support structures with an overhanging geometry parallel to the XY plane rather than on inclined surfaces. They employed block supports to facilitate simplicity and enhance comprehension of the impacts seen during studies. The results indicated that hatching factors impact support structures significantly more than tooth factors. Dimopoulos et al. [16] evaluated the thermal behavior of various support structures and optimized the designs to minimize support volume and residual stress while maintaining high-quality prints during LPBF. They evaluated several support structures, including blocks, lines, contours, and cones, to find the best strategies for reducing support volume and residual stress without sacrificing print quality. The results showed that the block supports had great thermal behavior. Weber et al. [17] employed tree-like support structures to evaluate the effect of design and laser powder bed fusion (L-PBF) parameters. They identified scanning speed and laser power as the most influential L-PBF parameters. In addition, it was found that the design parameters of stem and branch diameter and the number of branches had the most significant impact on the structural qualities. Strano et al. [18] introduced an innovative methodology for designing support structures that enhance the orientation of the build section and the configuration of the support cellular structure. Wang et al. [19] investigated the overhanging structural fabrication capabilities of selective laser melting for 316L stainless steel parts. They determined that in overhanging constructions beyond the crucial inclination angle, the support line should be designed according to the slicing slope, utilizing a tooth profile with a higher contact rate at the base to ensure effective operation. Hussein et al. [20] investigated the feasibility of using cellular support structures to support selective laser sintering for metallic parts. They validated their technique by conducting some exploratory experiments and conducting more studies based on their early findings [21]. Investigating two forms of lattice structures, the gyroid and the diamond, for their appropriateness as support structures, the results demonstrate that the structural needs may be satisfied with less material and building time spent. In addition, cellular support systems have demonstrated the capability to sustain metallic parts and mitigate part deformation. White et al. [22] introduced a computational framework that helps with the design of lattice support structures, using stochastic optimization to maximize heat dissipation for LPBF. The results show that the framework is valid by producing optimum hybrid lattice support structures for a cantilever beam, outperforming the uniformly distributed benchmark design by around 16% while still meeting manufacturing restrictions. Additionally, White et al. [23] presented a modified simulated annealing technique for developing lattice structures using laser powder bed fusion by optimizing the distribution of a library of diverse unit cell types, resulting in hybrid lattice support structures. The results demonstrate that the technology can meet production restrictions while saving up to 62% in post-processing costs and 61% in material costs compared to a solid support domain. Concerning residual stress and the time needed for support removal, Sulaiman et al. [24] optimized the parameters of the contour support structure, which include contour offset, teeth height, teeth top length, and teeth base length, for AlSi10Mg SLM parts. The findings demonstrate that contour offset substantially affects the magnitude of residual stress and the duration needed for support removal, whereas all factors are relevant for support volume. For minimal residual stress, the optimal parameters are a contour offset of 0.6 mm, a height of 1.4 mm, a top length of 0.75 mm, and a base length of 1.55 mm of teeth. Table 1 summarizes the reported studies on the

AM technology-based block support structure for metal parts. These studies showed that support structure design in AM is crucial for enhancing the performance of fabricating high-quality parts to satisfy the requirements of sustainable manufacturing.

Machine learning (ML) is an effective method for constructing industrial models, especially for monitoring and predicting manufacturing process performance. ML is a field of artificial intelligence that develops models or systems that can learn from data and make predictions or take actions. Artificial neural networks (ANN) and adaptive neuro-fuzzy inference systems (ANFISs) are part of a family of machine learning (ML) algorithms and have achieved more accurate outcomes compared with traditional methods in developing models [25–29]. Several researchers have adapted artificial intelligence techniques such as ANNs and ANFISs to enhance multi-objective optimization and guarantee reliable results in manufacturing processes, primarily because these processes are highly complex and nonlinear [30–32]. For example, Abbas et al. [33] integrated the Edgeworth–Pareto approach with ANNs to optimize the optimization of milling parameters, reducing the time spent on machining and improving surface integrity. Based on the effective results of the ANFIS method, Alqahtani et al. [30] used this method to enhance the quality of micromachining performance. In the milling of titanium alloys with difficult-to-machine surfaces, energy efficiency and tool wear may be predicted and optimized using the hybrid technique proposed by Xi et al. [34], which combines radial basis function with ANN and MOPSO models. The data clearly show the efficacy of the proposed strategy. Deb and Jain [35] developed a multi-objective NSGA-II approach, designated NSGA-III, which exhibits improved efficacy in addressing problems with more than two objectives. The implementation of NSGA-III demonstrated its superiority in generating efficient optimal solutions across several objectives. Nasr and Anwar [36] developed an intelligent method, utilizing improved NSGA-III with AI-based ANFIS to enhance the performance of the post-processing EBM parts. Their research demonstrates significant promise for employing developed predictive models, utilizing artificial intelligence and the combined ANFIS models in an improved NSGA-III method to improve the precision of the intricate turning process.

A recent trend in manufacturing process optimization emphasizes hybrid optimization techniques that integrate artificial intelligence modeling methods (e.g., ANN, ANFIS) with metaheuristic algorithms (e.g., PSO, GA, MOPSO, NSGA–II, and NSGA–III) to identify optimal process parameters for improved performance. In the realm of additive manufacturing, several contributions have emerged in the literature on the EBM technique. A few contributions concerning the EBM technique have appeared in the literature in the additive manufacturing area. Saleem [37] proposed in her thesis that the Support Vector Machine (SVM) and ANN methods can be used to predict the EBM parameters. Regarding the other AM technology, several researchers proposed machine learning models to predict the AM process performance [38–41]. For example, Khalad et al. [42] explored a data-driven machine learning approach for optimizing process parameters of the laser powder bed fusion (L-PBF) process. As a result, they found that gradient boosting with particle swarm optimization was the most effective way of predicting L-PBF performance. To predict the best process parameters for pressureless sintering and photopolymerization-based 3D printing, Singh et al. [43] proposed the use of ANNs and regression models. The results showed that the ANN model demonstrated superior predictive performance. To enhance the quality of fabricated 316L stainless steel parts, Hodroj et al. [44] used machine learning techniques based on ANN, SVM, and AdaBoost to predict SLM part density and optimize SLM parameters. These parameters include scan speed, laser power, hatch spacing, and layer thickness. According to the findings, the AdaBoost model outperformed others in terms of density prediction accuracy. Consequently, there is growing interest in developing intelligent models based on ML to address complex issues while providing dependable

outcomes. ML models based on artificial intelligence are being constructed to achieve precise outcomes when modeling highly complex nonlinear processes.

Table 1. Summary of studies conducted on metallic support structure that relies on AM technology.

Ref.	Materials/3D Printing Technology	Study Objectives	Type of Support/Design Support Parameters/BM Parameters	Type Study	Machine Learning Models
[45]	EBM	Developing a model to simulate the deformation of overhang parts during 3D printing of EBM parts.	Design type/design parameters	Explore study	No
[5]	Ti6Al4V/EBM	Investigating how the process parameters and support design impacted the support volume and overhangs.	Design parameters/EBM parameters	Single approach at the time	No
[8]	Ti6Al4V/EBM	Studying the influence of building settings and EBM parameters on warping deformation.	EBM parameters	Statistical analysis	No
[46]	Ti6Al4V/EBM	Studying the effect of design and process parameters of the perforated block support structures.	Perforated block structure parameters and EBM parameters	Statistical analysis/RSM with GA	No
[47]	Ti6Al4V/EBM	Designing support structures for metal AM that are easy to remove and consume less support material.	fragmented support structures and EBM parameters	Statistical analysis/RSM with MOGA-II	No
[48]	Inconel 718/LPBF	Investigating the influence of support geometries on the mechanical characteristics of Inconel 718 overhang parts.	Different support geometries	Single approach at the time	No
[17]	LPBF	They evaluated the support structure type and its design parameters.	Support structure type design parameters	Statistical analysis based on Taguchi design	No
[24]	AlSi10Mg/SLM	Optimizing the contour support structure parameters on residual stress and the time required for support removal.	Support structure parameters	Optimization	No
[12]	TiAl6V4/SLM	Examining the properties of various support structures.	Support structure parameters	NA	No
[15]	IN625/DMLS	The initial series of tests investigating the influence of Block supports dimensions.	Different support structure design	NA	No
[49]	L-BPF	Optimizing the tree-like support structure parameters.	Different support structure parameters	Optimization based on the Advanced Meta-model	No

It is evident from the literature review that support structure design and their parameters, as well as AM technologies parameters, are the major challenges enhancing the performance of the fabricated parts. It also found that integrating intelligent models that combine the three phases involved in fabricating the parts—design block structure type, block structure design parameters, and AM technologies processing parameters—remains an obstacle in the domain of additive manufacturing technologies. Recently, machine learning (ML) models have been particularly effective and represent a new trend in manufacturing that seeks to reduce costs and conserve time, emerging as a practical approach.

Furthermore, no information is provided regarding the monitoring, prediction, and optimization of the performance of the block support structure, which is one of the major challenges when processing 3D-printed parts (see Table 1) using MLs. Wadea et al. [46,47] explored the influence of support structure design with EBM parameters on the support block structure's performance. However, their research did not consider the integration of three phases (design block structure type, block structure design parameters, and AM technologies' processing parameters). Additionally, no study has been conducted to predict and optimize the performance of the support structures of AM technologies for AM in general, and EBM in particular, using an integrated hybrid ANFIS-ANN with the NSGA-III method. This would combine block structure type, block structure design parameters, and EBM parameters to fulfill the smart manufacturing requirements. This study focuses on machine learning models, utilizing AI-ANFIS, AI-ANN, and the improved NSGA-III technique to monitor, predict, and enhance the quality of produced parts, reduce material wastage, and reduce the post-processing time of fabricated EBM Ti6Al4V parts. To achieve this, an RSM-based regression model was first used to study the influence of block support structure type, design parameters, and EBM parameters. Secondly, statistical analysis was developed to provide a detailed analysis of the influence of the design block structure type and its interaction with design parameters and EBM parameters on warping deformation, support volume, and support volume time, which is not covered in the previous study by Wadee [5,46,47]. Thirdly, AI-ANFIS and AI-ANN models are designed to monitor and predict the performance of the support structure. Finally, machine learning models based on the AI-ANFIS technique with the high-performance NSGA-III optimization method were developed to obtain an optimal support structure type while enhancing the quality of produced parts (less warping deformation), reducing material wastage (less support volume), and reducing the post-processing time of fabricated EBM Ti6Al4V parts (less support volume type). This research intends to develop a machine learning system to enhance EBM's quality and economic performance by integrating the design and processing stages.

2. Methodology

This work provided statistical analysis to study the effect of design type, design parameters, and EBM parameter interactions. The aim was to enhance the block structure's performance. Monitoring, predicting, and optimizing WD, SRT, and SV during the fabrication of EBM parts is achieved by developing ML models that integrate hybrid ANFIS and ANN with an advanced NSGA-III optimization method. Figure 2 shows the methodology proposed in the current study.

2.1. Production and Measurements Scheme

A detailed description of the block support design and fabrication process is presented in previous work [47], which can be summarized as follows: a block support structure is designed with dimensions of 15 mm length, 10 mm width, and 5 mm thickness using Magics software, as shown in Figure 3.

This study examines the fragmented block support (F) and perforated block support (P) types, along with design parameters (tooth height and tooth base interval) and process parameters (beam current and scan speed), as shown in Figure 4a,b.

Titanium alloy (Ti6Al4V), with an average particle diameter of approximately 75 μm, is utilized in powder form to fabricate the EBM parts in the current investigation. The chemical composition of Ti6Al4V powder consists of Al (5.16%), V (4.40%), and Pt (4.01%), with the remainder being Ti, expressed in weight percentage. The ARCAM A2 machine was employed to fabricate the test specimens, as seen in Figure 5. In the EBM process, the produced electron beam fuses the metal alloy powder into a substantial part layer-by-layer.

Standard process settings for a 50μ layer of Ti6Al4V alloy are employed in the production of the test specimens. The ARCAM firm specifies the optimum process parameters as follows: a beam spot diameter of 200 μm, a layer penetration depth of 1.5, a current of 15 mA, a scan speed of 4530 mm/s, a focus offset of 3 mA, and a line offset of 0.1 mm.

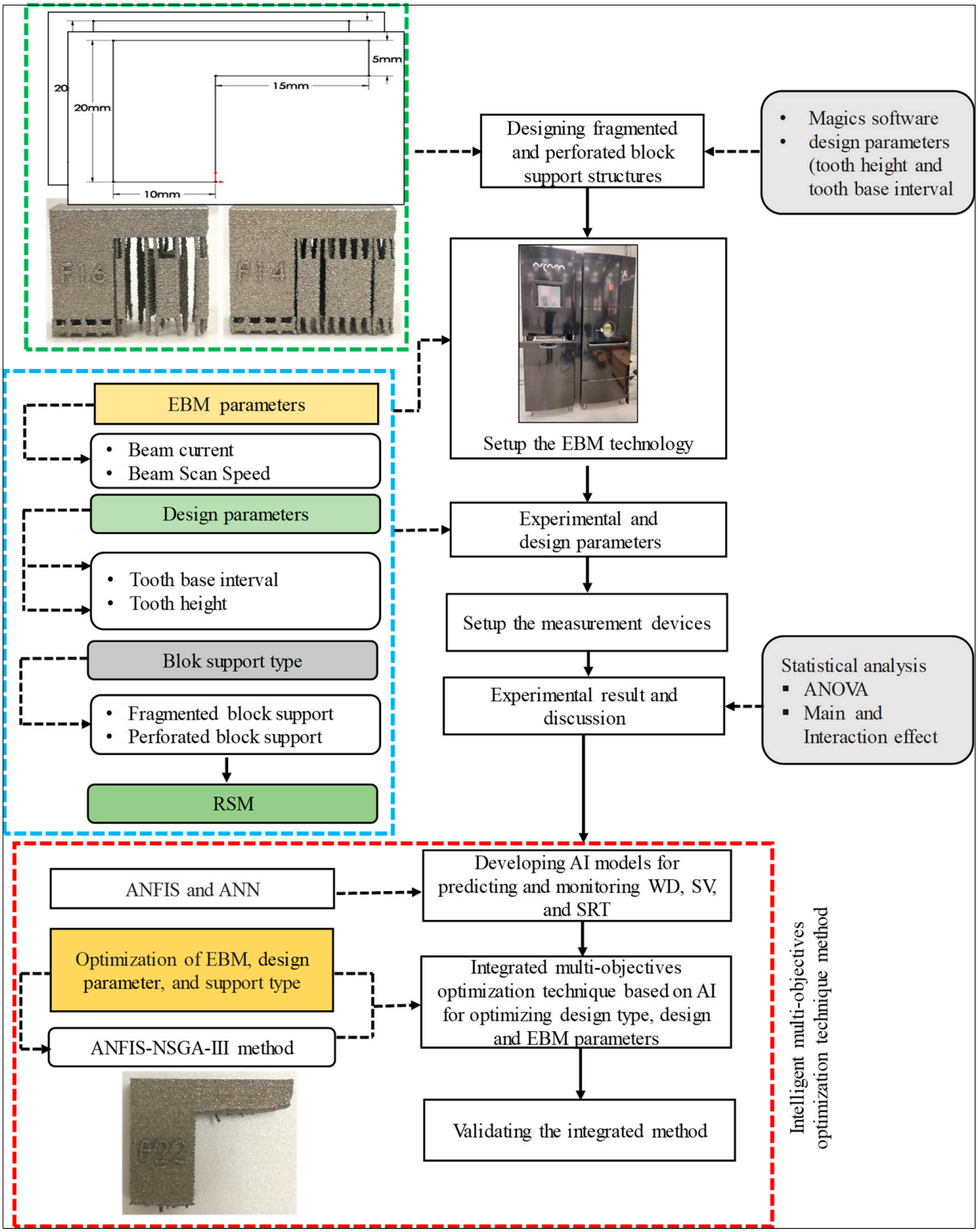


Figure 2. Methodology developed to enhance quality and efficiency of fabricated EB.

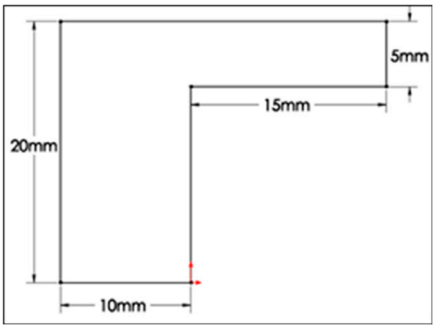


Figure 3. Testing specimen dimensions.

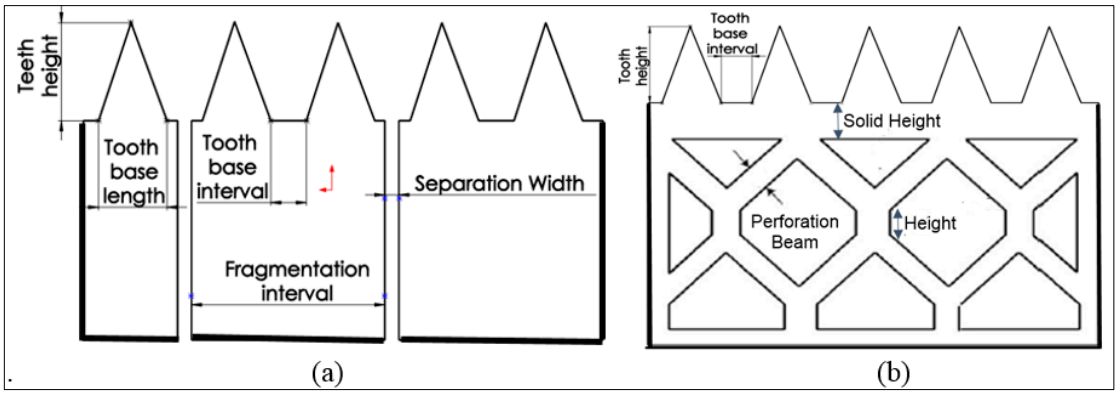


Figure 4. Block support parameters: (**a**) fragmented and (**b**) perforated support parameters.

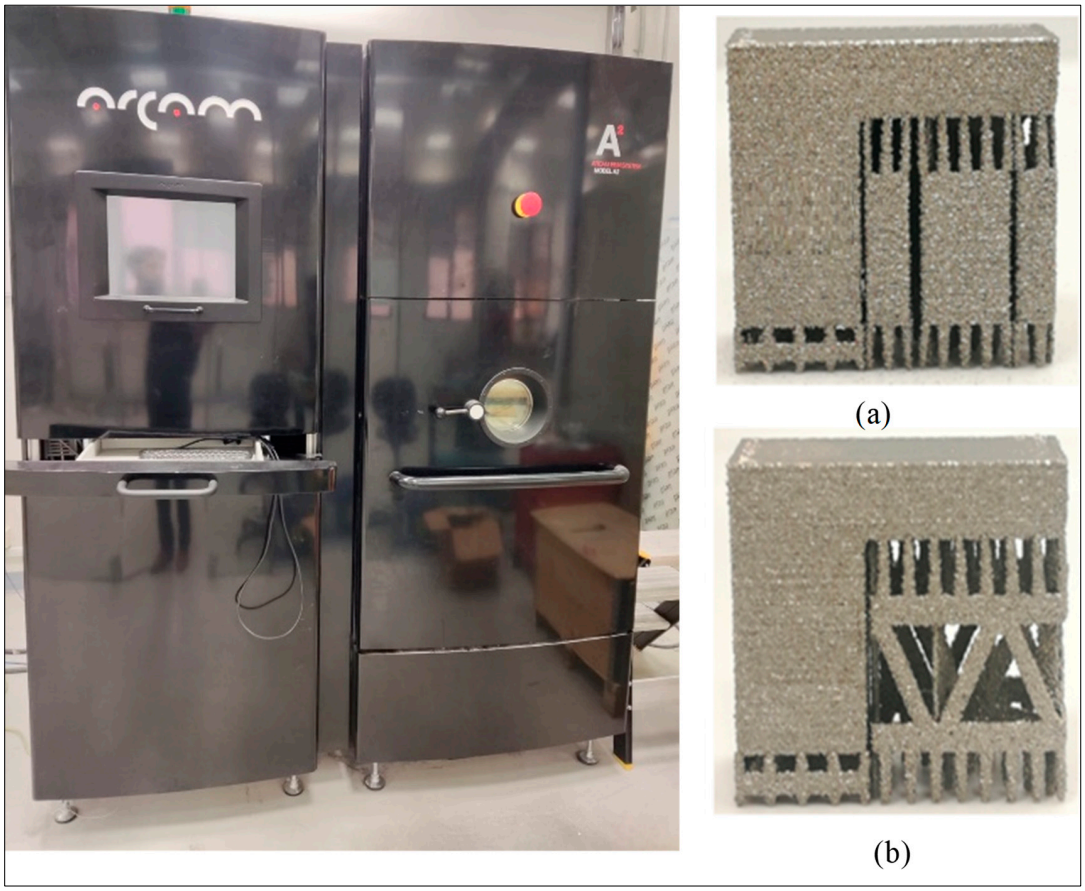


Figure 5. ARCAM technology setup with produced parts: (**a**) overhang with fragmented support structures; (**b**) overhang with perforated support structures.

The DOE approach is employed to plan and carry out experiments and assess the outcomes. Response surface methodology (RSM) is used to design experiments. Table 2 delineates the support factors together with their respective levels. In addition to the values of 2.5 mm Th, 2.5 mm Tb, 3.75 mA Bc, and 1600 mm/s Bss were chosen as the center points of each parameter. We set the number of sampling points to 34 and the number of fabricated specimens per point to 3. These levels were selected based on the previous work. In previous work, the chosen parameters were used to study the influence of parameterization and and optimize support structure parameters and EBM parameters in terms support volume, support volume type, and warping deformation using the traditional method (regression models with the MOGA method). However, their works did not consider the integration of three phases (design block structure type, block structure design parameters, and EBM processing parameters). The present study is an extension of the work of Wadea et al. [46,47], which works to statistically analyze the effect of block support structure types and how they interact with parameter design and EBM processing parameters on the performance of block support structures. In addition, a robust machine learning-based multi-optimization method that integrates the AM design (type and parameters) and EBM printing is needed to improve the quality of EBM parts, reduce material wastage, and improve the efficiency of removal support time. Three performance metrics are used to evaluate and enhance the performance of specified block support structures: support volume (SV), support removal time (SRT), and overhang warping deformation (WD). The volume of the supporting structure is quantified utilizing the STL viewer. The STL viewer is a specialized online tool for viewing CAD models developed or exported in the STL file format. To evaluate the support removability, the produced samples undergo the process of support structure elimination upon removal from the unmelted powder. The support structures are physically removed with basic pliers, and the time taken to remove each specimen is recorded (SRT). Upon the completion of specimen fabrication and the removal of support structures, the specimens are assessed for deformation. The shadowgraph technique, utilizing a profile projector, assesses the specimen's deformation (W.D).

Table 2. Block support structures type, design parameters, EBM parameters, and their levels.

Parameter	Level 1	Level 3
Tooth height (Th) (mm)	1	4
Tooth base interval (Tbi) (mm)	1	4
Beam current (BC) (mA)	1.5	6
Beam scan speed (Bss) (mm/s)	1200	2000
Block support type	Fragmented (1)	Perforated (2)

Consequently, the RSM models are employed to study the influence of design support structure type, design parameters, and EBM parameters, along with their interactions, on the performance of specified block support structures to enhance the quality of the EBM parts produced. Using analysis of variance (ANOVA) and a 95% confidence interval, statistical analysis was conducted to determine how different factors affect support removal time, support volume, and overhang warping deformation. The *p*-value was utilized for the parameters and their interactions to check for statistical significance. Minitab 17 was used to conduct statistical analysis. The built models' accuracy is evaluated using the coefficient of determination (R^2).

2.2. ML Models with Improved NSGA-III Method

We will develop AI models based on ANFIS and ANN techniques to monitor the quality of the fabricated parts and predict the support volume and support removal time to overcome the limitations of traditional methods. Integrated hybrid AI models evaluate the performance of block support structures and how well a combination of three stages satisfies the criteria for the performance of specified block support structures simultaneously. AI-ANFIS and an improved NSGA-III approach were designed for multi-objective optimization to enhance the performance of specified block support structures. Figure 6 depicts the comprehensive framework of the hybrid ANFIS developed and the improved NSGA-III method.

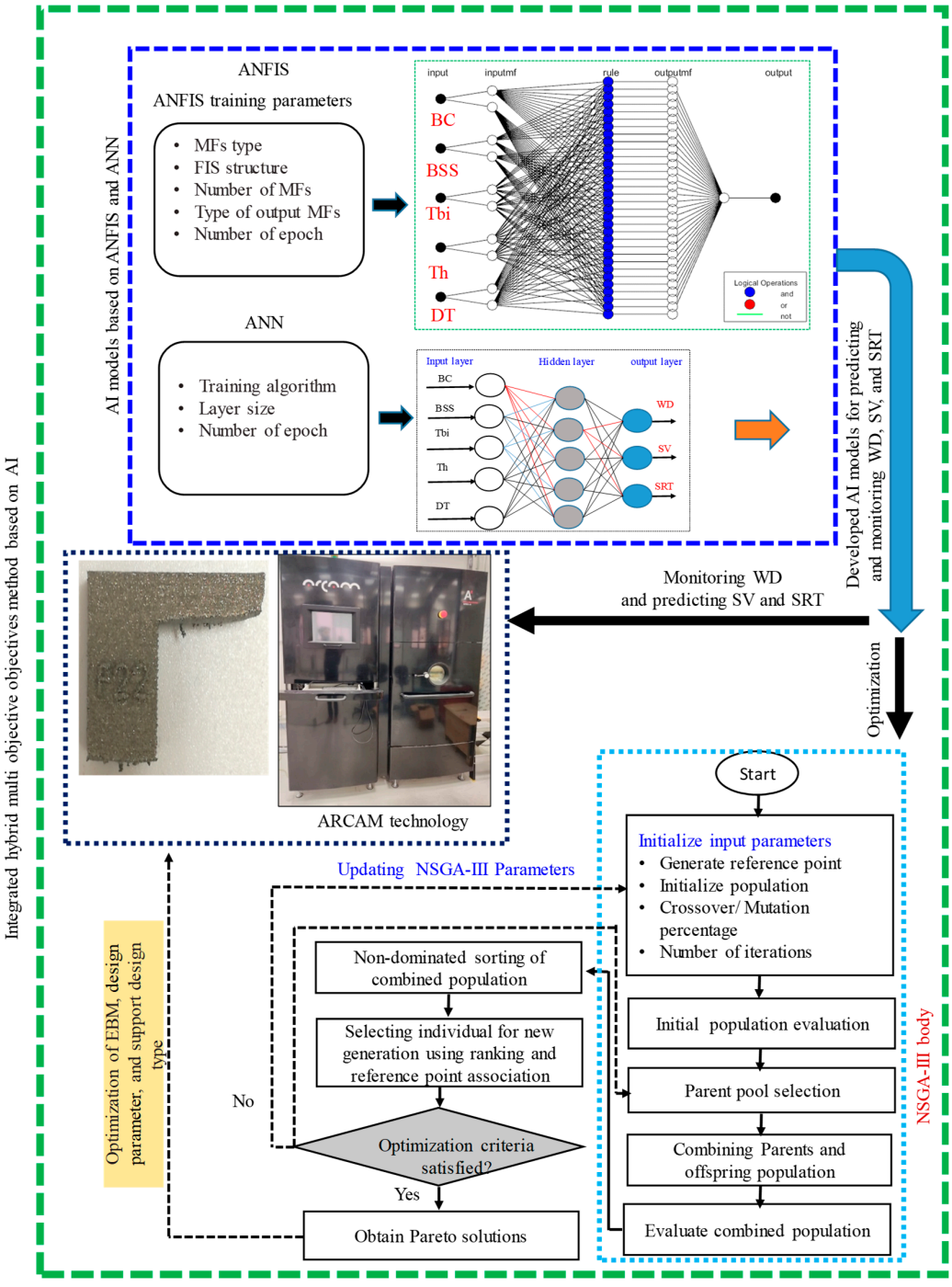


Figure 6. Framework of developed intelligent method utilizing ANFIS and improved NSGA-III.

2.2.1. AI-ANFIS Models

Artificial intelligence-based ANFIS and ANN can provide solutions to support structural design and EBM in processing nonlinear and complex problems. Specifically, fuzzy inference systems (FISs) and artificial neural networks (ANNs) are parts of the hybrid system known as ANFIS. According to [50], an FIS comprises five layers, with different node functions characterizing each layer. Figure 4 (ANFIS structure) illustrates the FIS structure with five inputs, each of which consists of two membership functions (MFs) for each input and one single output. These AI models are used to model the nonlinear support structure type and their parameters, as well as the EBM processing parameters. NSGA III can employ these models as its fitness function to carry out the optimization process. Matlab 2023b was utilized in the development of the ANFIS. The specifications of the computer used to running the algorithm are a RAM of 16.0 GB, a 13th Gen Intel(R) Core(TM) i7-1355U 1.70 GHz processor, and 500 GB SSD.

The ANFIS algorithm has two phases: the training phase and the testing phase. The training process begins with the establishment of the ANFIS algorithm, as shown in Figure 6, which includes the types of membership functions (MFs), the structure of the fuzzy inference system (FIS), the number of MFs, the type of output MFs, the number of epochs, and the training optimization approach. The training procedure will persist in adjusting the training parameters until the least MSE is achieved. Thereafter, the verified data will be utilized to evaluate the accuracy of the built AI models in predictions or to modify the ANFIS parameters to determine the optimal learning parameters. Figure 7 illustrates a sample of the learning curve. These machine learning algorithms may be employed to assess the quality of electron beam melting parts. These ML models can be used to monitor the quality of EBM parts in case of warping deformation. The number of epochs is selected based on the minimum RMSE.

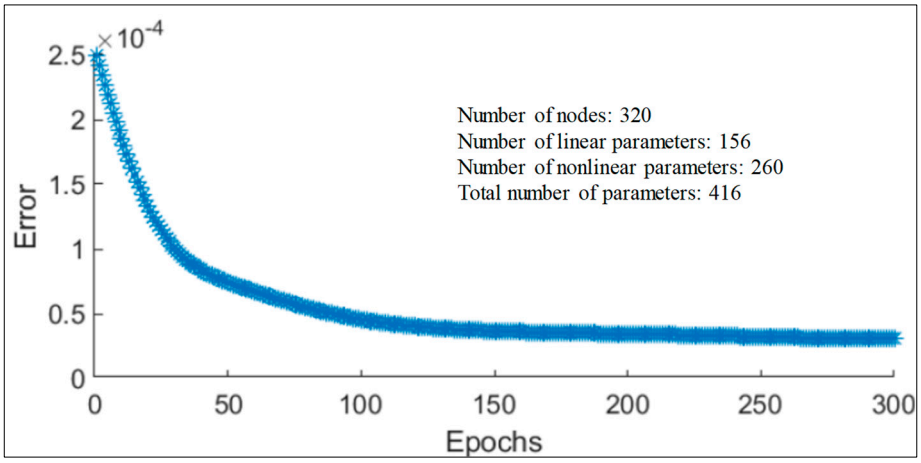


Figure 7. Learning curve of support removal time.

2.2.2. AI-ANN Models

One kind of computational model is an artificial neural network (ANN), which is designed to emulate human neurons' functioning to train a computer. The construction of an artificial neural network involves three layers, each comprising distinct neurons. The three layers consist of the input, hidden, and output layers. The input layer denotes a layer of neurons where data is first configured, whereas the hidden layer comprises neurons that remain concealed without disclosing data. The output layer is the neuronal layer that encompasses the acquired data in need of retrieval. Figure 6 shows a network diagram with a single neuron (ANN diagram). The ANN Toolbox in MATLAB 2024b was utilized to construct machine learning models based on artificial neural networks. This study

examines a model including five inputs and three outputs. The acquired experimental data was divided to train the network, after which the trained network was evaluated using the remaining datasets. The parameters of the ANN algorithm will be specified, as shown in Figure 6, to start the training process. These parameters include the following: the training algorithm type—Levenberg–Marquardt or Bayesian regularization; the scaled conjugate gradient; the layer size; and the number of epochs. The training procedure will adjust the parameters until the minimum mean squared error (MSE) is achieved. In Figure 8, the training curve for SV is displayed.

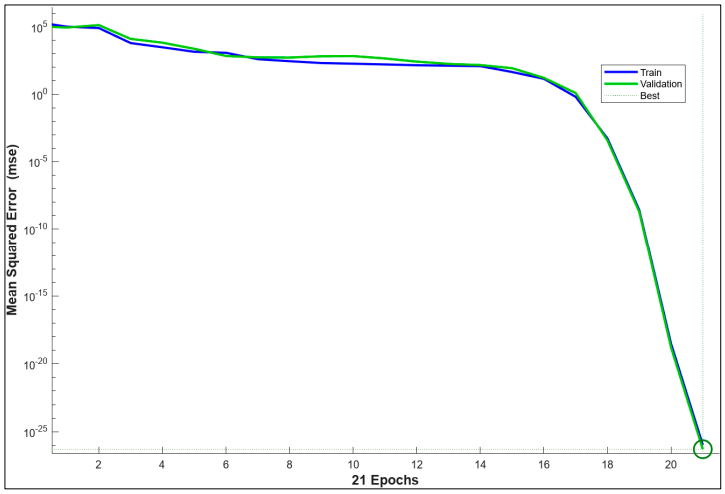


Figure 8. Training curve for SV.

The mean absolute percentage error is calculated as follows equation to evaluate the predicted models using ANFS, ANN, and the regression models:

$$\text{MAPE} = \frac{1}{n}\sum_{t=1}^{n}\left|\frac{\text{Experimental value} - \text{predicted value}}{\text{Experimental value}}\right| \quad (1)$$

2.2.3. Improved NSGA-III Method

This section will integrate the dominated sorting genetic algorithm (NSGA-III) method with the developed ML based on ANFIS. The improved NSGA III algorithm has better convergence and diversity than other methods, which have proved superior to other methods in performance. In their proposal of the non-dominated sorting genetic algorithm (NSGA), Srinivas and Deb [51] used a ranking technique and a non-dominated sorting operation to identify and endeavor to preserve reasonable solutions in the population. An updated version of the NSGA, NSGA-II, was developed by Deb et al. [52] The updated method is more efficient computationally, avoids elitism, and maintains diversity with less dependence on a sharing parameter. It executes NSGA quickly. Continuing with the reference-point-based multi-objective outlook from NSGA-II, Deb and Jain [35] developed the NSGA-III method. For issues with more than two objectives, this approach performs better. One of the novel features of NSGA-III is the use of reference points. These points can be either a collection of known or consciously constructed ones.

Recently, there has been an increasing demand for using advanced tools to enhance the performance of multi-objective optimization of complex manufacturing problems. Several researchers reported studies using the advanced NSGA-II approach to ensure a globally optimal solution for improving the multi-objective optimization of nonlinear manufacturing behavior, such as machining problems [53–58]. However, multi-objective optimization also depends on the prediction models that are developed. These models were developed using the traditional method, which achieved high errors. Therefore, employing

ML models based on ANFIS as fitness functions yielded more precise outcomes than the traditional technique during the optimization process. These models will enhance the efficiency of the optimization-based NSGA-III method. The method presented by Nasr and Anwar [36] improve the integrated the advanced NSGA-III algorithm with a machine learning (ML)-based AI tool to address issues with support structure design during EBM processing. Figure 4 depicts the major body of the NSGA-III algorithm. The steps of the NSGA-III algorithm are described in detail [35,53]. This was achieved by utilizing the ANFIS-based approach integrated with the NSGA III technique for multi-response optimization, which improved the performance of the support structure design through the use of fitness functions developed by the ANFIS approach. The constraints of block support structure design type and their parameters, as well as the EBM process, are constructed as follows:

$$1 \leq T_h \leq 4\text{mm}$$
$$1 \leq T_{bi} \leq 4\text{mm}$$
$$1.5 \leq Bc \leq 6\text{mA}$$
$$1200 \leq Bss \leq 2000\text{mm/s}$$
$$\text{Let } x \in \{1, 2\} \textit{ denote the Blok support type, where :}$$
$$x = 1 + y,\ y \in \{0, 1\}$$
This enforces :

- $x = 1\ if\ y = 0$ ($Blok\ support\ type$ 1)
- $x = 2\ if\ y = 1$ ($dBlok\ support\ type$ 2)

Blok support type: fragmented and perforated (block support type is integer 1 or 2).

The initial stage in each optimization process is adjusting the NSGA-III algorithm's parameters (initialized population, reference point crossover percentage, mutation percentage). The NSGA-III settings will be updated, and the Pareto solution set will be utilized to evaluate the objective functions until the convergence characteristics of NSGA-III are obtained. Additionally, the ANFIS parameters are revised to further enhance the NSGA-III results' convergence.

3. Results and Discussion

3.1. Statistical Analysis Based on ANOVA

Tables 3–5 show all support structure performance ANOVA results after eliminating insignificant interaction factors using a backward technique. Tables 3–5 show that all factors with p-values < 0.05 significantly affect WD, SRT, and SV. Furthermore, the design type substantially influences the quality of the printed parts (DW) and the volume of support material. Additionally, the interaction between design type (DT) and design parameter (tooth height, Th) significantly impacts printed part quality. Furthermore, the indicated interaction terms significantly impact support structure performance.

R-squared values, both adjusted and predicted, are computed from the model. All replies have a high R-squared value, indicating that these models adequately describe over 75% of the variation in the selected performance outputs. The models' capability for predicting DW is insufficient regarding the R-squared predicted, with a value of 60.55%. However, models with complex methods, like ML-based AI, are required to build models. The developed regression equations for each response are presented as follows.

$$W.D = -0.318 + 0.2364 \times DT - 0.0053 \times Th + 0.0332 \times Tb - 0.267\ Bc + 0.000704 \times Bss + 0.0447 \times Bc^2 \quad (2)$$

$$srt = 3.6 - 1.95 \times dt - 8.94 \times th - 1.16 \times tb + 24.21 \times bc - 0.00759 \times bss + 1.446 \times th^2 - 2.138\ th \times bc \quad (3)$$

$$SV = 2464.18 - 819.32 \times DT - 223.77 \times Th + 0.05 \times Tb + 0.008 \times Bc + 0.00069 \times Bss + 125.64\ DT \times Th \quad (4)$$

Table 3. Results of the ANOVA for DW.

Source	DF	Adj SS	Adj MS	F	*p*-Value
DT	1	0.47159	0.47159	10.28	0.004
Th	1	0.00199	0.00199	0.04	0.837
Tb	1	0.07849	0.07849	1.71	0.202
Bc	1	2.02616	2.02616	44.15	0.000
Bss	1	0.39634	0.39634	8.64	0.007
Square	1	0.09634	0.09634	2.1	0.159
Bc×c	1	0.09634	0.09634	2.1	0.159
2-way interaction	1	0.32264	0.32264	7.03	0.013
Bc×Bss	1	0.32264	0.32264	7.03	0.013
Total	33	4.89574			

R-squired = 75.63%, R-predicted = 60.55.

Table 4. Results of the ANOVA for SV.

Source	DF	Adj SS	Adj MS	F-Value	*p*-Value
DT	1	2,161,342	2,161,342	67,192.96	0.00
Th	1	251,140	251,140	7807.58	0.00
Tb	1	40,695	40,695	1265.15	0.00
Bc	1	0	0	0	0.986
Bss	1	2	2	0.07	0.788
2-way interaction	2	297,216	148,608	4620	0.00
DT×Th	1	283,018	283,018	8798.6	0.00
Th×Tb	1	14,709	14,709	457.29	0.00
Total	33	2,762,064			

R-squired = 99.97%, R-predicted = 99.96%.

Table 5. Results of the ANOVA for SRT.

Source	DF	Adj SS	Adj MS	F	*p*-Value
DT	1	31.8	31.84	1.13	0.299
Th	1	1976.4	1976.41	70.17	0.00
Tb	1	1095	1095.02	38.88	0.00
Bc	1	7793.5	7793.46	276.69	0.00
Bss	1	819	819	29.08	0.00
2-way interaction	5	3854.6	770.92	27.37	0.00
Th×Tb	1	334.4	334.36	11.87	0.002
Th×Bc	1	1644.8	1644.79	58.39	0.00
Th×Bss	1	283.7	283.73	10.07	0.004
Tb×Bc	1	1040	1040.02	36.92	0.00
Bc×Bss	1	570.5	570.5	20.25	0.00
Total	33	16,294.5			

R-squared = 96.02%, R-predicted = 90.97%.

The ANOVA obtained the main effect and interaction plots for support structure performance (WD, SV, and SRT), as shown in Figures 9–11. As seen from the interaction effect plot in Figure 9a,b, the design type (Fragmented type) obtained less deformation (WD) than the perforated design. In addition, with the raising of the beam current (Bc) from 2 mA to 4 mA, the WD decreased and then slightly increased with increasing Bc to 6 mA. Moreover, when raising the Bc from 2 to 6 mA and simultaneously reducing the beam scan speed (Bss) from 2000 mm/s to 1200 mm/s, the WD decreased and then slightly increased.

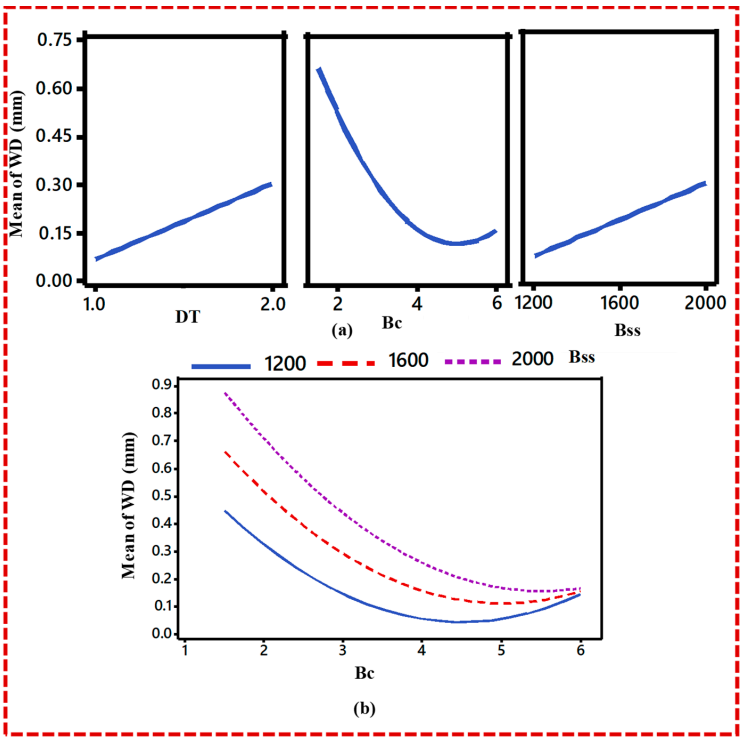


Figure 9. Main effects and interaction plots for WD.

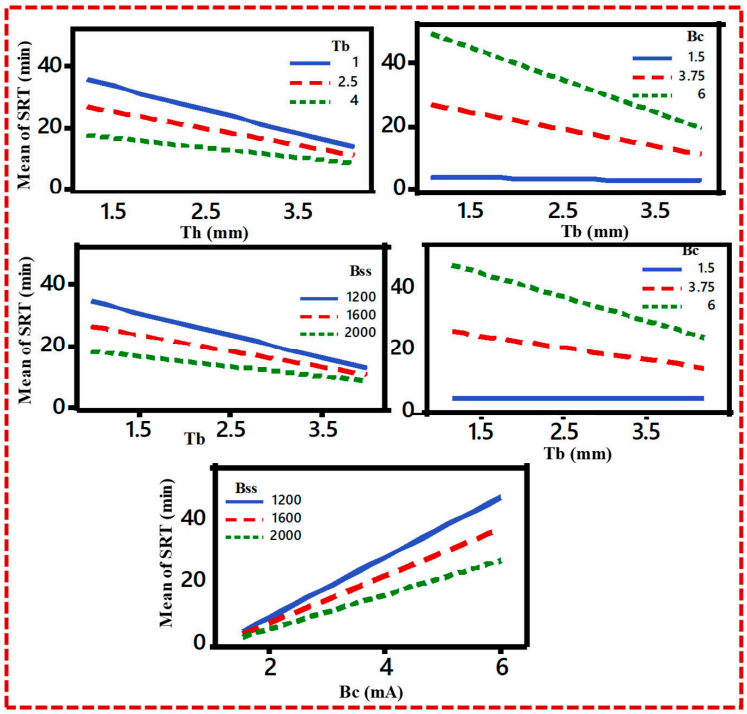


Figure 10. Main effects plots for SRT.

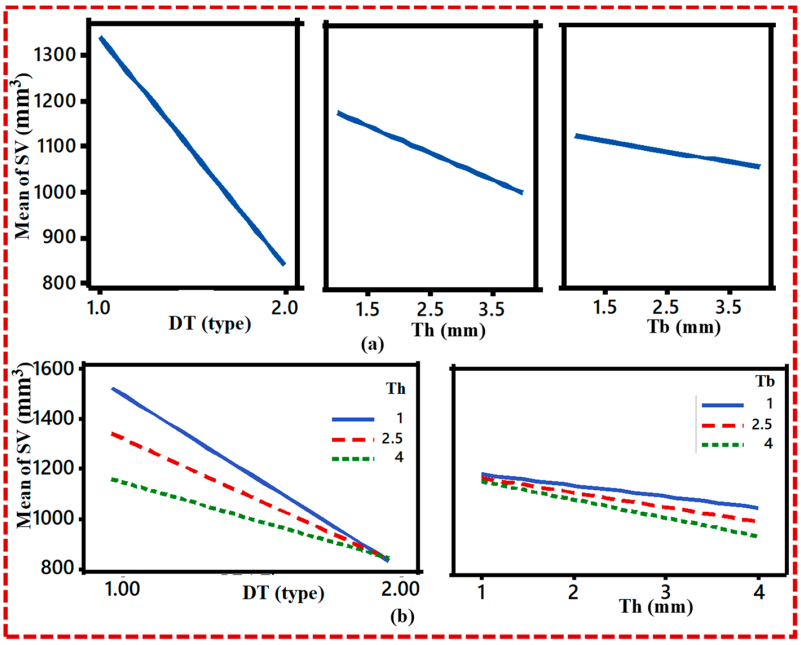


Figure 11. Main effects and interaction plots for SV.

Regarding the effect of main and interaction terms on SRT, as shown in Figure 11a, the Bc, at a high level of 2 mA, and Bss, at a high level of 2000 mm/s, presented a low support removal time. Moreover, the design parameters of Tb and the high level of 3.5 mm showed the lowest removal time.

Regarding the effect of main and interaction terms on SV, as shown in Figure 11b, the design type with a fragmented design obtained an increase in support volume of approximately 60% compared with a perforated design. In addition, by raising the Tb and Th from 1.5 mm to 3.5 mm, the SV decreased. The reasons are explained in the previous work [47]. The interaction plots show that the interaction between the design type (DT) and the Th and Tb presented the lowest support volume when the design type was fragmented, and the Th increased from 1 to 4. It can be concluded that the design type, its parameters, and the EBM parameters affect the performance support structure.

3.2. Artificial Intelligence Models Based on the ANFIS and ANN Approaches

This section will use the AI intelligent system to monitor and predict the quality of the printed parts. This employs the following parameters: warping deformation (WD), support volume (SV), and support removal time (SR). An AI-based intelligent system was designed utilizing ANFIS and ANN. Through the utilization of training and testing data that was separated by the results of the experiments, effective ANFIS and ANN models were achieved. In other words, the models were constructed using training data and then tested with testing data. For this research, the ANFIS algorithm was adapted to support multiple outputs. The ANFIS algorithm was trained to minimize the RMSE by adjusting the fuzzy inference parameters. Regarding the FIS parameters that were selected to achieve the lowest RMSE, please refer to Table 6. The design of experiments (single approach at a time) was used to select the values of the subclustering squash factor, accept ratio, and reject ratio to avoid overfitting. We will choose the values for each variable that yield the smallest RMSE. A number of epochs were identified by the minimum RMSE errors (see learning curve in Figure 7).

Table 6. FIS parameters.

Training Optimization Method	WD	SV	SRT
	Hybrid Method	**Hybrid Method**	**Hybrid Method**
Generated FIS	Subclustering	Grid partition	Subclustering
MFs type	Subclustering with a range of influence = 0.7	Trimf	Subclustering with a range of influence = 0.3
	Squash factor = 1		Squash factor = 1.2
	Accept ratio = 0.5		Accept ratio = 0.3
	Reject ratio = 0.1		Reject ratio = 0.09
Number of MFs	29 29 29 29 29	2 2 2 2 2	26 26 26 26 26
Type of output MFs	NA	Constant	NA
Number of epochs	120	20	100

Conversely, AI based on the ANN technique was proposed to evaluate the effectiveness of the ANFS models developed. An ANN algorithm was trained until it obtained the lowest RMSE, with several changes in layer size parameter and training algorithm type. Table 7 presents the best parameters for the ANN algorithm, which obtained the lowest RMSE. The parameters for ANN training were determined using a design of experiments approach, focusing on one variable at a time to achieve the lowest RMSE. We will choose the values for each variable that yield the smallest RMSE.

Table 7. ANN training parameters.

Training Algorithm	Wd	SV	SRT
	Levenberg–Marquardt	**Levenberg–Marquardt**	**Levenberg–Marquardt**
layer size	3	3	5
Number of epochs	16	29	27

Consequently, the FIS and ANN algorithms were trained utilizing the designated training parameters provided in Tables 6 and 7, respectively. Figure 12 depicts the experimental data for both the training and testing stages. The values were compared to the predicted values from ANFIS, ANN, and regression models for the warping deformation, WD, support volume (SV), and support removal time (SR). As shown in Figure 12, the precision of the constructed ANFIS models is demonstrated by the closeness of the differences between the experimental and predicted values using ANFIS for all responses. In the case of SV, ANN, and regression models, the closeness of the differences between the experimental values and the ANN and regression predicted values is demonstrated. In addition, to ensure the effectiveness of AI-ANFS models, Figure 13 compares the validation experimental values and values predicted by ANFIS. It is found that the predicted values with ANFIS closely align with the validated values.

Furthermore, to enhance the effectiveness of ANFIS models, it is essential to validate their performance by comparing them with ANN and regression models. TMAPE was utilized to assess the constructed models' efficacy. The mean MAPE for each output response is presented in Table 8 for the ANFIS, ANN, and regression models. Table 9 presents the MAPE for both the training and testing stages. In the case of WD and SRT, the MAPE of the ANFIS is significantly lower than that of the ANN and regression models. ANN and regression models were shown to have the most significant errors for WD and

SRT, with 50%, 55.97%, 21.04%, and 11.2%, respectively. Conversely, the ANFIS models had the fewest errors, reaching a rate of 1.28%, which is the lowest error rate out of those compared. The present circumstances may illustrate that ANFIS models are dependable and capable of precisely delivering a fitness function for the NSGA III intelligent methodology. The present scenario may prove that ANFIS models are trustworthy and provide an adequate fitness function for the NSGA III intelligent approach.

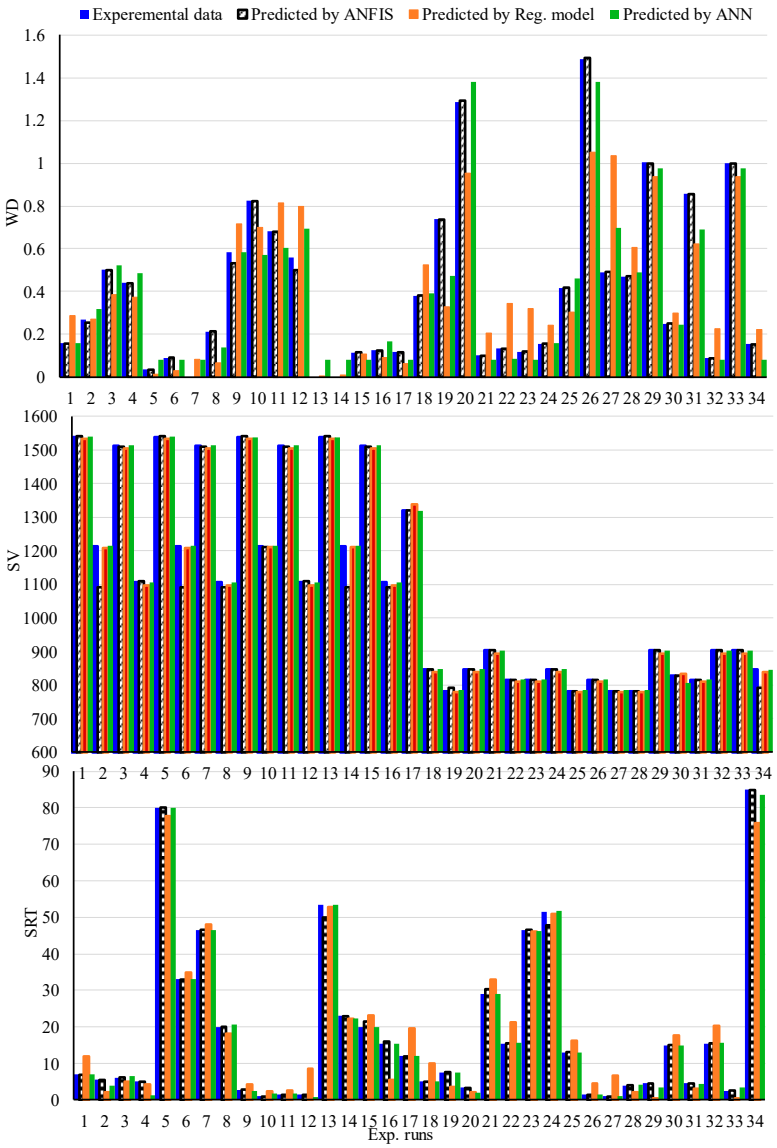


Figure 12. Comparison of experimental data with predicted ANFIS, ANN, and regression values.

Table 8. Models' performance on training and test data.

Block Support Structure Performance	ANFIS Model	ANN Model	Reg. Model
	MAPE	MAPE	MAPE
WD	0.992%	21.04%	50.33%
SRT	1.28%	11.2%	55.97%
SV	1.2%	1.21%	1.98%

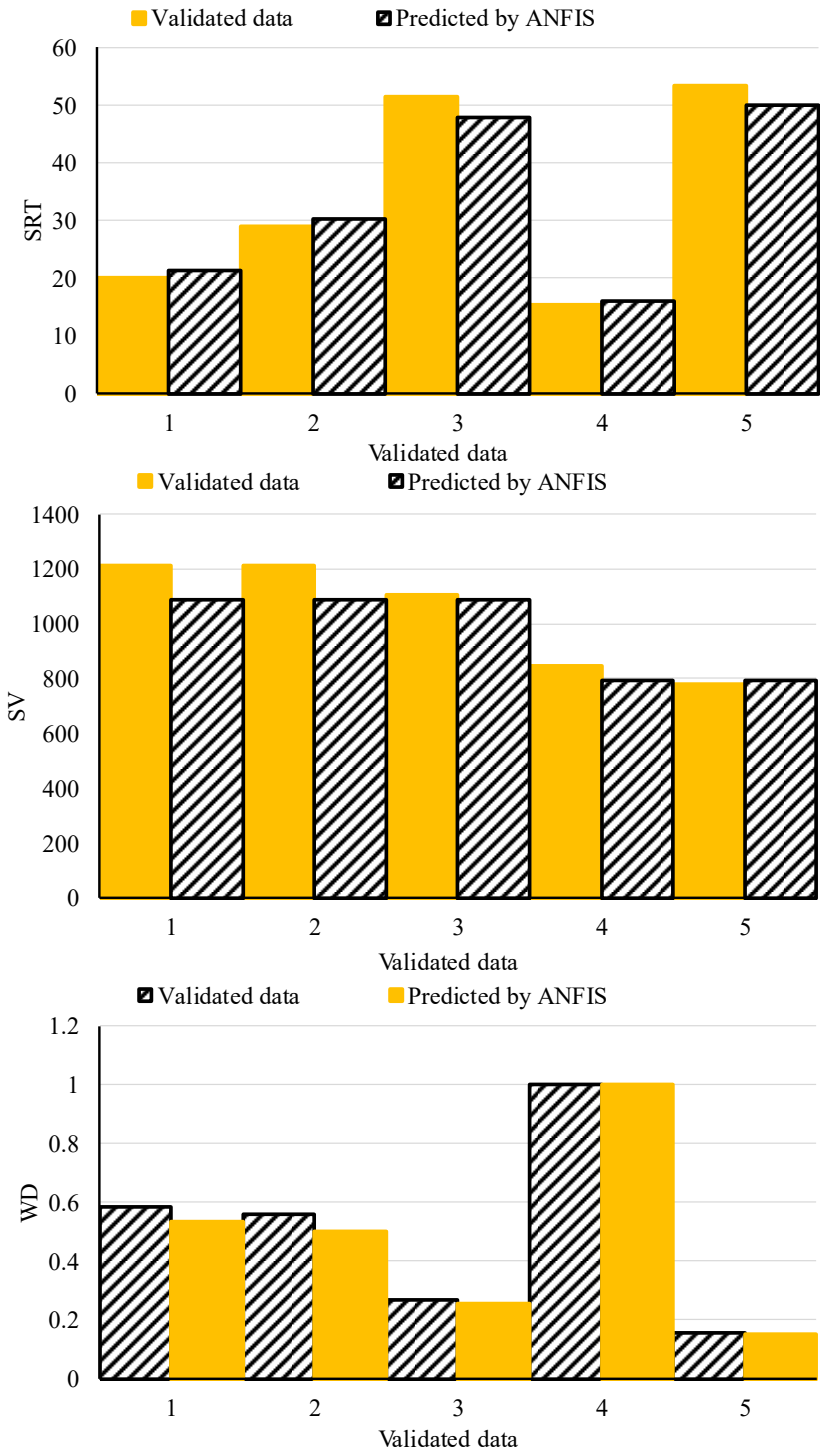


Figure 13. Evaluating validity of ANFIS values by comparing them to experimental values.

Table 9. Settings for NSGA III.

Parameters	Values
Population size	80
Mutation percentage	0.5%
Mutation rate	0.02
Number of iterations	100
Crossover percentage	0.6%

3.3. Machine Learning-Based Multi-Objective Optimization

This section uses multi-objective optimization to print high-quality parts with low warping deformation, less material waste, and removal support time. For optimal support structure performance, a single design type, design parameters, and EBM parameters are required. To achieve this, ANFIS-based multi-response optimization was combined with the NSGA III method, using fitness functions developed by ANFIS using the specified parameters. The technique section describes the optimization's block structure, EBM constraints, and NSGA III settings. Table 9 shows the optimized NSGA III parameters.

After finishing the optimization process, the best feasible combination that integrates block support design type, design parameters, and EBM parameters was achieved to fabricate high-quality EBM parts with enhanced support block structure performance. Table 10 displays the possible solutions that might enhance the performance of the block support structure that leads to lower warping deformation, a minimum support volume (less material wastage), and a minimum amount of time required to remove the support. Additional tests were conducted under optimal conditions to evaluate the dependability and accuracy of the recently developed ANFIS-NSGA III approach. The confirmed trials were carried out, and Table 10 displays the outcomes of the comparisons. The ANFIS-NSGA III approach has a lower MAPE (less than 6.5%), indicating the integrated technique's effectiveness and increased efficiency. Several researchers compared the most up-to-date methods for multi-objective optimization to the hybrid ANFIS-NSGA III approach [54,56,59–61]. These modern methods included Support Vector Machine regression (SVR), ANN-NSGA-II-ETOPSIS and NSGA-III, NSGA-II, and adaptive geometry estimation (AGE-MOEA). With MAPE values ranging from 2.4% to 6.4% across the board, the ANFIS-NSGA III approach clearly outperformed state-of-the-art approaches. Moreover, the block support structure was optimized using a regression-based desirability function to verify further the reliability and accuracy of the developed ANFIS-NSGA III. The results obtained are presented in Table 10. It can be observed that the regression-based desirability function shows MAPE values ranging from 0.44% to 55.7%, which is a higher error than that of ANFIS-NSGAIII. A total of 18.28 s was required for the ANFIS-NSGA III to complete its execution.

Table 10. Optimal combination with validated experiments of an integrated support structure type with their parameters and EBM parameters.

		DT	Th	Tb	Bc	Bss	DT	SRT	SV
		Type	mm	mm	mA	mm/s	mm	s	mm^3
ANFIS-NSGA III	Optimized results	2	1	1	1.5	1200	0.361	5.32	825
		2	3.98	1.2	2.95	1200	0.271	6.73	774
		2	3.21	1.452	2.3	1400	0.242	3.27	825.31
	Validated results	2	1	1	1.5	1200	0.3797	5	846
						MAPE	4.92	6.4%	2.4%
Desirability Function	Optimized results	2	4	4	5.98	2000	0.3266	3.497	784.453
	Validated results	2	4	4	6	2000	0.7375	7.5	781
						MAPE	55.7%	53.37%	0.44%

4. Conclusions

Support structures are required to produce overhang structures using electron beam melting, yet their incorporation leads to increased manufacturing time, greater requirements for materials, extra effort, and a more complex engineering procedure. While commercial software can automatically design support structures, it frequently produces excessive support, increasing material usage, extended processing time, and elevated post-processing costs. This research aims to optimize the block support structure type and the design of their parameters and EBM parameters to enhance their performance, increase the quality of the produced parts (less WD), lower material usage (less SV), and support post-processing (less SRT). This study uses RSM-based statistical analysis to detail the influence of design type (fragmented, perforated), design parameters (tooth height (Th) and tooth base interval (Tb)), and EBM parameters (beam current (Bc), beam scan speed (Bss)) on block support structure performance during the EBM printing of Ti6Al4V. The use of ANOVA looked at how the design type (fragmented, perforated), design parameters, and EBM parameters and their interaction influenced the efficiency and quality of fabricated EBM parts. In addition, intelligent models based on ANN and ANFIS have been constructed to monitor, predict, and obtain optimal design types, design parameters, and EBM parameters. An integrated advanced NSGA-III method with AI-based constructed models was developed to enhance block structure performance further. This technique accurately represents the realistic behavior of the process under conditions where all responses change simultaneously with the change in design type and EBM parameters, which could not be accomplished by using a single factor at a time. The findings below provide a more detailed summary.

- According to the statistical study results, DT, Bc, and Bss strongly impacted the warping deformation. Another important factor influencing the warping distortion of EBM parts during manufacturing was the interaction between Bc and Bss. In order to regulate warping deformation, design type (DT), Bc, and Bss are crucial. DT mainly caused variations in SV of 78% and in Th of 9%, and interaction between Th and DT was approximately 10%. Th, DT, and the interplay of Th, DT, Th, and Tb also played a significant role in the warping distortion. Th, Tb, Bc, and Bss all substantially impact the SRT, as is the case with their interactions, according to the ANOVA data.
- An ML-based intelligent system utilizing the ANFIS and ANN approaches has been developed to monitor and predict warping deformation, SV, and SRT during the EBM fabrication of parts. With MAPE values of 0.992%, 1.2%, and 1.28%, respectively, the ANFIS model correctly predicted WD, SR, and SRT. The ANFIS models showed 95.22%, 0.826%, and 83.92% improvements in the accuracy of WD, SV, and SRT, respectively, compared to the ANN models. Furthermore, the ANFIS models showed a decrease in errors of 98% for WD, 96.78 for SV, and 39.39% for SRT compared to regression models. The results demonstrate that the AI-ANFIS model outperforms the ANN AND regression model in terms of accuracy and reliability in predicting block support structure performance.
- During EBM part fabrication, ANFIS modeling and advanced NSGA-III multi-objective optimization significantly improved block support structure performance. A fragmented type of design structure, with Th of 1 mm, Tb of 1 mm, Bc of 1.5 mA, and Bss of 1200 mm/s mm, may provide higher quality (less warping deformation), minimal material utilization (SV), and lower SRT by optimizing design type, design parameters, and EBM parameters. Consequently, it can produce high-quality EBM parts in a cleaner environment, achieving less wasteful material utilization and lower post-processing time.

This work demonstrates tremendous potential for improving the accuracy of the block support structure while 3D printing Ti6Al4V using EBM parts and the AI-based prediction models constructed utilizing the approach combining ANFIS with the NSGA-III.

Author Contributions: Conceptualization, W.A. and M.M.N.; methodology, W.A. and M.M.N.; software, M.M.N. and W.A.; validation, W.A. and A.D.; formal analysis, W.A. and M.M.N.; investigation, W.A.; resources, A.A.-A.; data curation, W.A.; writing—original draft, M.M.N., W.A. and A.D.; Writing—review and editing, W.A., M.M.N., A.D. and A.A.-A.; supervision, A.A.-A.; project administration, A.A.-A.; funding acquisition, A.A.-A. All authors have read and agreed to the published version of the manuscript.

Funding: Raytheon Chair for Systems Engineering for funding.

Data Availability Statement: The original contributions presented in this study are included in the article. Further inquiries can be directed to the corresponding author.

Acknowledgments: The authors would like to thank the Raytheon Chair for Systems Engineering for funding.

Conflicts of Interest: The authors declare no conflicts of interest.

References

1. Vayre, B.; Vignat, F.; Villeneuve, F. Metallic Additive Manufacturing: State-of-the-Art Review and Prospects. *Mech. Ind.* **2012**, *13*, 89–96. [CrossRef]
2. Ameen, W.; Al-Ahmari, A.; Mohammed, M.K.; Abdulhameed, O. Evaluation of the Support Structure Removal Techniques for Additively Manufactured Ti6AL4V Parts. *Adv. Mater. Sci. Eng.* **2022**, *2022*, 2259974. [CrossRef]
3. Gan, M.X.; Wong, C.H. Practical support structures for selective laser melting. *J. Mater. Process. Technol.* **2016**, *238*, 474–484. [CrossRef]
4. Jiang, J.; Stringer, J.; Xu, X. Support Optimization for Flat Features via Path Planning in Additive Manufacturing. *3D Print. Addit. Manuf.* **2019**, *6*, 171–179. [CrossRef]
5. Ameen, W.; Mohammed, M.K.; Al-Ahmari, A.; Ahmed, N.; Mian, S.H. Investigation of Support Structure Parameters and Their Affects during Additive Manufacturing of Ti6Al4V Alloy via Electron Beam Melting. *Proc. Inst. Mech. Eng. Part L J. Mater. Des. Appl.* **2020**. [CrossRef]
6. Shen, Z.-H.; Dai, N.; Li, D.-W.; Wu, C.-Y. Bridge Support Structure Generation for 3D Printing. In *Materials, Manufacturing Technology, Electronics and Information Science*; World Scientific Publishing: Singapore, 2016; pp. 141–149. [CrossRef]
7. Calignano, F. Design Optimization of Supports for Overhanging Structures in Aluminum and Titanium Alloys by Selective Laser Melting. *Mater. Des.* **2014**, *64*, 203–213. [CrossRef]
8. Ameen, W.; Al-Ahmari, A.; Ahmed, N.; Alshammary, W.; Salunkhe, S.; Hussein, H.M.A. Investigation the Effect of Electron Beam Melting Parameters on Overhang Structure Deformation. *Mater. Technol.* **2022**, *37*, 1586–1593. [CrossRef]
9. Vaidya, R.; Anand, S. Optimum Support Structure Generation for Additive Manufacturing Using Unit Cell Structures and Support Removal Constraint. *Procedia Manuf.* **2016**, *5*, 1043–1059. [CrossRef]
10. Dijkstra, E.W. A Note on Two Problems in Connexion with Graphs. *Numer. Math.* **1959**, *1*, 269–271. [CrossRef]
11. Järvinen, J.P.; Matilainen, V.; Li, X.; Piili, H.; Salminen, A.; Mäkelä, I.; Nyrhilä, O. Characterization of Effect of Support Structures in Laser Additive Manufacturing of Stainless Steel. *Phys. Procedia* **2014**, *56*, 72–81. [CrossRef]
12. Lindecke, P.N.J.; Blunk, H.; Wenzl, J.P.; Möller, M.; Emmelmann, C. Optimization of Support Structures for the Laser Additive Manufacturing of TiAl6V4 Parts. *Procedia CIRP* **2018**, *74*, 53–58. [CrossRef]
13. Allen, S.; Dutta, D. *On the Computation of Part Orientation Using Support Structures in Layered Manufacturing*; The University of Texas at Austin: Austin, TX, USA, 1994.
14. Wei, W.; Wu, H.; Zhang, J.; Zhang, M.; Yuan, L.L.; Zhou, Z.; Long, Y. Model Decomposition Method for Minimizing the Consumption of Support Structure for FFF. *J. Manuf. Process.* **2025**, *133*, 395–407. [CrossRef]
15. Poyraz, Ö.; Yasa, E.; Akbulut, G.; Orhangül, A.; Pilatin, S. *INVESTIGATION OF SUPPORT STRUCTURES FOR DIRECT METAL LASER SINTERING (DMLS) OF IN625 PARTS*; University of Texas at Austin: Austin, TX, USA, 2015.
16. Dimopoulos, A.; Salimi, M.; Gan, T.H.; Chatzakos, P. Support Structures Optimisation for High-Quality Metal Additive Manufacturing with Laser Powder Bed Fusion: A Numerical Simulation Study. *Materials* **2023**, *16*, 7164. [CrossRef]
17. Weber, S.; Montero, J.; Bleckmann, M.; Paetzold, K. PARAMETERS on SUPPORT STRUCTURE DESIGN for METAL ADDITIVE MANUFACTURING. *Proc. Des. Soc. Des. Conf.* **2020**, *1*, 1145–1154. [CrossRef]

18. Strano, G.; Hao, L.; Everson, R.M.; Evans, K.E. A New Approach to the Design and Optimisation of Support Structures in Additive Manufacturing. *Int. J. Adv. Manuf. Technol.* **2013**, *66*, 1247–1254. [CrossRef]
19. Wang, D.; Yang, Y.; Zhang, M.; Lu, J.; Liu, R.; Xiao, D. Study on SLM Fabrication of Precision Metal Parts with Overhanging Structures. In Proceedings of the IEEE International Symposium on Assembly and Manufacturing (ISAM), Xi'an, China, 30 July–2 August 2013; pp. 222–225. [CrossRef]
20. Hussein, A.; Yan, C.; Everson, R.; Hao, L. Preliminary Investigation on Cellular Support Structures Using SLM Process. In *Innovative Developments in Virtual and Physical Prototyping, Proceedings of the 5th International Conference on Advanced Research and Rapid Prototyping, Leiria, Portugal, 28 September–1 October 2011*; Taylor Francis Group: London, UK, 2012; pp. 609–612. [CrossRef]
21. Hussein, A.; Hao, L.; Yan, C.; Everson, R.; Young, P. Advanced Lattice Support Structures for Metal Additive Manufacturing. *J. Mater. Process. Technol.* **2013**, *213*, 1019–1026. [CrossRef]
22. White, L.; Liang, X.; Zhang, G.; Cagan, J.; Zhang, Y.J. Coupling Simulated Annealing and Homogenization to Design Thermally Conductive Hybrid Lattice Support Structures for LPBF. In Proceedings of the ASME 2023 International Design Engineering Technical Conferences, Boston, MA, USA, 20–24 August 2023; Volume 2. [CrossRef]
23. White, L.; Liang, X.; Zhang, G.; Cagan, J.; Zhang, Y.J. A Modified Simulated Annealing-Based Method for Hybrid Lattice Support Structure Design in LPBF Additive Manufacturing. *J. Comput. Inf. Sci. Eng.* **2024**, *24*, 121002. [CrossRef]
24. Sulaiman, M.R.; Yusof, F. Effect of Support Structure Design toward Residual Stress of Part Build Using Selective Laser Melting: Auswirkung Des Stützstrukturdesigns Auf Die Restspannung Des Bauteilaufbaus Unter Verwendung Des Selektiven Laserstrahlschmelzens. *Mater. Werkst.* **2023**, *54*, 1138–1147. [CrossRef]
25. Savkovic, B.; Kovac, P.; Dudic, B.; Rodic, D.; Taric, M.; Gregus, M. Application of an Adaptive "Neuro-Fuzzy" Inference System in Modeling Cutting Temperature during Hard Turning. *Appl. Sci.* **2019**, *9*, 3739. [CrossRef]
26. Alajmi, M.S.; Almeshal, A.M. Prediction and Optimization of Surface Roughness in a Turning Process Using the ANFIS-QPSO Method. *Materials* **2020**, *13*, 2986. [CrossRef]
27. Mikołajczyk, T.; Nowicki, K.; Bustillo, A.; Pimenov, D.Y. Predicting Tool Life in Turning Operations Using Neural Networks and Image Processing. *Mech. Syst. Signal Process.* **2018**, *104*, 503–513. [CrossRef]
28. Wang, H.Z.G. Improved NSGA-III Using Transfer Learning and Centroid Distance for Dynamic Multi-Objective Optimization. *Complex Intell. Syst.* **2023**, *9*, 1143–1164. [CrossRef]
29. Ghosh, T.; Martinsen, K. Generalized Approach for Multi-Response Machining Process Optimization Using Machine Learning and Evolutionary Algorithms. *Eng. Sci. Technol. Int. J.* **2020**, *23*, 650–663. [CrossRef]
30. Alqahtani, K.N.; Nasr, M.M.; Anwar, S.; Al-Samhan, A.M.; Alhaag, M.H.; Kaid, H. Integrated Intelligent Method Based on Fuzzy Logic for Optimizing Laser Microfabrication Processing of GnPs-Improved Alumina Nanocomposites. *Micromachines* **2023**, *14*, 750. [CrossRef]
31. Choudhary, A.; Kumar, M.; Gupta, M.K.; Unune, D.K.; Mia, M. Mathematical Modeling and Intelligent Optimization of Submerged Arc Welding Process Parameters Using Hybrid PSO-GA Evolutionary Algorithms. *Neural Comput. Appl.* **2020**, *32*, 5761–5774. [CrossRef]
32. Tran, H.C.; Lo, Y.L. Systematic Approach for Determining Optimal Processing Parameters to Produce Parts with High Density in Selective Laser Melting Process. *Int. J. Adv. Manuf. Technol.* **2019**, *105*, 4443–4460. [CrossRef]
33. Abbas, A.T.; Pimenov, D.Y.; Erdakov, I.N.; Mikolajczyk, T.; Soliman, M.S.; El Rayes, M.M. Optimization of Cutting Conditions Using Artificial Neural Networks and the Edgeworth-Pareto Method for CNC Face-Milling Operations on High-Strength Grade-H Steel. *Int. J. Adv. Manuf. Technol.* **2019**, *105*, 2151–2165. [CrossRef]
34. Xi, L.; Li, L.; Li, L.; Zhao, J.; Sutherland, J.W. Parameter Optimization of Titanium Alloy Considering Energy Efficiency and Tool Wear Based on RBFNN-MOPSO Algorithm in Milling. *J. Manuf. Process.* **2024**, *122*, 97–111. [CrossRef]
35. Deb, K.; Jain, H. An Evolutionary Many-Objective Optimization Algorithm Using Reference-Point-Based Nondominated Sorting Approach, Part I: Solving Problems with Box Constraints. *IEEE Trans. Evol. Comput.* **2014**, *18*, 577–601. [CrossRef]
36. Nasr, M.M.; Anwar, S. Developing an Intelligent Approach Based on ANFIS and Advanced NSGA-III for Improving the Turning Performance of Additively Manufactured γ-TiAl Alloy. *Int. J. Adv. Manuf. Technol.* **2025**, *137*, 3333–3358. [CrossRef]
37. Saleem, B. Characterization of the EBM Additive Manufacturing Process Parameters Using Artificial Neural Networks. Master's Thesis, Politecnico di Torino, Torino, Italy, 2020.
38. Costa, A.; Buffa, G.; Palmeri, D.; Pollara, G.; Fratini, L. Hybrid Prediction-Optimization Approaches for Maximizing Parts Density in SLM of Ti6Al4V Titanium Alloy. *J. Intell. Manuf.* **2022**, *33*, 1967–1989. [CrossRef]
39. Cao, Y.; Chen, C.; Xu, S.; Zhao, R.; Guo, K.; Hu, T.; Liao, H.; Wang, J.; Ren, Z. Machine Learning Assisted Prediction and Optimization of Mechanical Properties for Laser Powder Bed Fusion of Ti6Al4V Alloy. *Addit. Manuf.* **2024**, *91*, 104341. [CrossRef]
40. Zhang, Y.; Cui, S.; Yang, B.; Wang, X.; Liu, T. Research on 3D Printing Concrete Mechanical Properties Prediction Model Based on Machine Learning. *Case Stud. Constr. Mater.* **2025**, *22*, e04254. [CrossRef]
41. Shafaie, M.; Khademi, M.; Sarparast, M.; Zhang, H. Modified GTN Parameters Calibration in Additive Manufacturing of Ti-6Al-4 V Alloy: A Hybrid ANN-PSO Approach. *Int. J. Adv. Manuf. Technol.* **2022**, *123*, 4385–4398. [CrossRef]

42. Khalad, A.; Telasang, G.; Kadali, K.; Zhang, P.N.; Xu, W.; Chinthapenta, V. A Generalized Machine Learning Framework for Data-Driven Prediction of Relative Density in Laser Powder Bed Fusion Parts. *Int. J. Adv. Manuf. Technol.* **2024**, *135*, 4147–4167. [CrossRef]
43. Singh, G.; Kumar, S.; Sharma, P. A Comparative Study of Artificial Neural Network and Regression Model for Hybrid Additive Manufacturing of Ti6Al4V Parts and Microstructural Analysis. *J. Mater. Eng. Perform.* **2024**, 1–12. [CrossRef]
44. Hodroj, A.; Bouglia, R.; Ding, Y.; Zghal, M. Machine Learning for Density Prediction and Process Optimization of 316L Stainless Steel Fabricated by Selective Laser Melting. *J. Intell. Manuf.* **2025**, 1–15. [CrossRef]
45. Cheng, B.; Chou, K. Geometric Consideration of Support Structures in Part Overhang Fabrications by Electron Beam Additive Manufacturing. *Comput. Des.* **2015**, *69*, 102–111. [CrossRef]
46. Ameen, W.; Mohammed, M.K.; Al-Ahmari, A.; Ahmed, N.; Dabwan, A.; Kaid, H. Optimization of Perforated Support Structures for Electron Beam Additive Manufacturing. *Int. J. Adv. Manuf. Technol.* **2022**, *120*, 7305–7323. [CrossRef]
47. Ameen, W.; Al-Ahmari, A.; Mohammed, M.K.; Kaid, H. Multi-Objective Optimization of Support Structures for Metal Additive Manufacturing. *Int. J. Adv. Manuf. Technol.* **2021**, *116*, 2613–2632. [CrossRef]
48. Gülcan, O.; Günaydın, K.; Çelik, A.; Yasa, E. Mechanical Properties of Laser Powder Bed Fusion Produced Overhang Parts with Different Support Geometries: An Experimental Study. *Prog. Addit. Manuf.* **2024**, *9*, 211–229. [CrossRef]
49. Weber, S.; Montero, J.; Bleckmann, M.; Paetzold, K. Parametric Design Optimisation of Tree-like Support Structure for the Laser-Based Powder Bed Fusion of Metals. *J. Manuf. Process.* **2022**, *84*, 660–668. [CrossRef]
50. Syukor, A.; Jaya, M.; Samad, A.; Basari, H.; Zaiton, S.; Hashim, M.; Muhamad, M.R.; Rahman, N.A. Application of ANFIS in Predicting of TiAlN Coatings Hardness Department of Industrial Computing, Faculty of Information and Communication Technology, Soft Computing Research Group (SCRG), Faculty of Computer Science and Information System, Departmen. *Aust. J. Basic Appl. Sci.* **2011**, *5*, 1647–1657.
51. Srinivas, N.; Deb, K. Muiltiobjective Optimization Using Nondominated Sorting in Genetic Algorithms. *Evol. Comput.* **1994**, *2*, 221–248. [CrossRef]
52. Deb, K.; Agrawal, S.; Pratap, A.; Meyarivan, T. A Fast Elitist Non-Dominated Sorting Genetic Algorithm for Multi-Objective Optimization: NSGA-II. In *Parallel Problem Solving from Nature-PPSN VI*; Lecture Notes in Computer Science; Springer: Berlin/Heidelberg, Germany, 2000; Volume 1917, pp. 849–858. [CrossRef]
53. Mobin, M.; Mousavi, S.M.; Komaki, M.; Tavana, M. A Hybrid Desirability Function Approach for Tuning Parameters in Evolutionary Optimization Algorithms. *Meas. J. Int. Meas. Confed.* **2018**, *114*, 417–427. [CrossRef]
54. Nguyen, V.H.; Le, T.T.; Nguyen, N.T.; Le, V.P.; Vu, T.L. Multi-Objective Optimization for Surface Roughness, Cutting Force, and Material Removal Rate During Turning 4340 Alloy Steel by Using Support Machine Vector and NSGA-III. In *Advances in Engineering Research and Application*; Lecture Notes in Networks and Systems (LNNS); Springer: Cham, Switzerland, 2024; Volume 944, pp. 132–140. [CrossRef]
55. Zhang, Z.; Wu, F.; Wu, A. Research on Multi-Objective Process Parameter Optimization Method in Hard Turning Based on an Improved NSGA-II Algorithm. *Processes* **2024**, *12*, 950. [CrossRef]
56. Nguyen, V.H.; Le, T.T.; Nguyen, A.T.; Hoang, X.T.; Nguyen, N.T. Multiobjective Optimization of End Milling Parameters for Enhanced Machining Performance on 42CrMo4 Using Machine Learning and NSGA-III. *Mach. Sci. Technol.* **2024**, *28*, 744–776. [CrossRef]
57. Amira, M.T.; Rezgui, I.; Belloufi, A.; Abdelkrim, M.; Touggui, Y.; Chiba, E.; Catalin, T.; Chiriță, B. Modeling and Multi-Objective Optimization of the Milling Process for AISI 1060 Steel. *Int. J. Adv. Manuf. Technol.* **2024**, *132*, 5705–5732. [CrossRef]
58. Ghadai, R.K.; Baraily, A.; Logesh, K.; Sapkota, G.; Patil, S.; Das, S.; Mandal, P. Objective Optimization of Drilling of Hybrid Aluminium Metal Matrix Composites Using ANN NSGA-II Hybrid Approach. *Int. J. Interact. Des. Manuf.* **2024**, *28*, 744–776. [CrossRef]
59. Feng, C.; Qin, E.; Li, W.; Li, M.; Su, J.; Xu, X. Energy Consumption and Surface Roughness Modelling for Multi-Objective Optimisation of Machining Processes. *Int. J. Adv. Manuf. Technol.* **2024**, *133*, 5065–5087. [CrossRef]
60. Goyal, A.; Gautam, N.; Pathak, V.K. An Adaptive Neuro-Fuzzy and NSGA-II-Based Hybrid Approach for Modelling and Multi-Objective Optimization of WEDM Quality Characteristics during Machining Titanium Alloy. *Neural Comput. Appl.* **2021**, *33*, 16659–16674. [CrossRef]
61. Yadav, S.K.; Ghosh, S.; Sivanandam, A. An Intelligent Hybrid Optimization Approach to Improve the End Milling Performance of Incoloy 925 Based on ANN-NSGA-II-ETOPSIS. *Int. J. Interact. Des. Manuf.* **2024**, *18*, 4673–4695. [CrossRef]

Disclaimer/Publisher's Note: The statements, opinions and data contained in all publications are solely those of the individual author(s) and contributor(s) and not of MDPI and/or the editor(s). MDPI and/or the editor(s) disclaim responsibility for any injury to people or property resulting from any ideas, methods, instructions or products referred to in the content.